

# Extraction of motor activity from the cervical spinal cord of behaving rats

Abhishek Prasad and Mesut Sahin

Department of Biomedical Engineering, New Jersey Institute of Technology, 323 MLK Blvd., Fenster Hall, Room 617, Newark, NJ 07102, USA

E-mail: [sahin@njit.edu](mailto:sahin@njit.edu)

Received 10 April 2006

Accepted for publication 30 August 2006

Published 18 September 2006

Online at [stacks.iop.org/JNE/3/287](http://stacks.iop.org/JNE/3/287)

## Abstract

Injury at the cervical region of the spinal cord results in the loss of the skeletal muscle control from below the shoulders and hence causes quadriplegia. The brain–computer interface technique is one way of generating a substitute for the lost command signals in these severely paralyzed individuals using the neural signals from the brain. In this study, we are investigating the feasibility of an alternative method where the volitional signals are extracted from the cervical spinal cord above the point of injury. A microelectrode array assembly was implanted chronically at the C5–C6 level of the spinal cord in rats. Neural recordings were made during the face cleaning behavior with forelimbs as this task involves cyclic forelimb movements and does not require any training. The correlation between the volitional motor signals and the elbow movements was studied. Linear regression technique was used to reconstruct the arm movement from the rectified–integrated version of the principal neural components. The results of this study demonstrate the feasibility of extracting the motor signals from the cervical spinal cord and using them for reconstruction of the elbow movements.

(Some figures in this article are in colour only in the electronic version)

## 1. Introduction

During spinal cord injury (SCI), axons of the upper motor neurons (descending fibers in the spinal cord) are cut and hence they lose their connection to the lower motor neurons that control the skeletal muscle. An injury at the cervical level results in quadriplegia with little function remaining in the arms. In these individuals, a method of generating voluntary command for environment control, self-mobility or computer access is extremely needed. These voluntary command signals may also be used to activate the person's own paralyzed muscles via electrical stimulation to regain function. The brain–computer interface (BCI) technique has demonstrated significant success in generation of command signals using neural activity recorded from the cortex [1–5]. As an alternative method, we are investigating the feasibility of using the motor signals recorded from the intact region of the cervical spinal cord above the point of injury.

In humans, there are two main descending (motor) systems in the brain that send down voluntary control signals to the spinal cord: the lateral descending system, whose axons

originate in the cortex and the magnocellular red nucleus, and the medial descending system. The medial descending system runs in the ventral funiculus of the spinal cord and mainly controls the axial and proximal limb (girdle) muscles. The lateral system communicates its axons through the dorsolateral funiculus of the spinal cord white matter and mainly provides the skillful control of the distal limb musculature. The lateral system consists of two major tracts: the lateral corticospinal tract (LCST) and the rubrospinal tract (RST).

The LCST and RST are closely interrelated at both supraspinal and spinal levels and may even terminate at the same site within the spinal cord in different species (reviewed in [6]). At the spinal level, they share common interneurons and propriospinal neurons [7, 8]. Both LCST and RST are located in the dorsolateral funiculus in close proximity to each other in humans. In rodents, the corticospinal tract (CST) arises from large pyramidal neurons in layer V of the sensorimotor cortex, passes through the ipsilateral medullary pyramid and subsequently travels in the contralateral dorsal column down to the most caudal level of the spinal cord [9]. It has been confirmed that the ventral-most portion of

the dorsal funiculus white matter contains the normal crossed CST [9–13]. In rodents, the uncrossed ventral CST is small at the cervical region [14–16] and cannot be traced below mid-thoracic levels [16].

The mammalian RST originates from the caudal or magnocellular division of the red nucleus [6, 12, 17, 18]. At the supraspinal level, it is well known that the red nucleus receives abundant cortical innervations both via direct corticobulbar cells and via collateral branches of pyramidal tract and corticospinal neurons. The RST fibers have also been shown to project ventrolaterally to a specific motoneuron population of the intermediate and distal muscles of the limbs [17].

In this study, the cervical spinal cord was chosen as the site of implantation for recording electrodes because of the involvement of the cervical cord in the control of distal, intermediate and proximal musculature for skilled forelimb movements in rats. A mid-cervical spinal injury (C5–C6) was assumed as a typical case of quadriplegia. Unlike humans, the CST and RST run in completely separate regions of the spinal cord cross-section in rats. This provides an opportunity to access these tracts separately with penetrating electrodes. Thus, microelectrode arrays were implanted either in the dorsal column or dorsolateral funiculus of the cervical cord for recordings of the CST or RST activity, respectively. Linear regression technique was applied to the delayed version of the principal components of the neural data to determine if the elbow movements could be reconstructed.

## 2. Methods

### 2.1. Materials

The microelectrode array (Cyberkinetics Neurotechnology Systems, Inc., UT) consisted of 12 silicon electrodes ( $4 \times 3$  configuration) on a  $2 \times 1.5$  mm<sup>2</sup> base. The electrode shanks were approximately 80  $\mu$ m wide at the base, 400  $\mu$ m apart and 1 mm long. Electrode tips had platinum coating to provide a low impedance electrical interface [19, 20]. Each of these electrodes was connected to a micro-connector (H2747-ND, Digi-Key Corp., MN) with a fine Pd–Au wire.

The flex sensor (Spectra Symbol, UT) used for recording the elbow joint movements was based on resistive carbon technology. The resistance of the sensor increased or decreased as a function of the bent angle and direction. A thin layer of silicone was applied to the sensor for electrical insulation and hermetic sealing. The silicone coating also facilitated the attachment of the sensor to the muscle tendons using non-absorbable sutures.

### 2.2. Surgical procedure

Four Long–Evans male rats, all weighing between 350 and 400 grams, were used in this study. The surgical procedures were approved by the Animal Care and Use Committee at Louisiana Tech University. A sterile surgery was performed to implant the microelectrode array and the elbow flex sensor.

Rats were anesthetized with pentobarbital sodium (Nembutal, 50 mg kg<sup>-1</sup>, IP) and deep anesthesia was

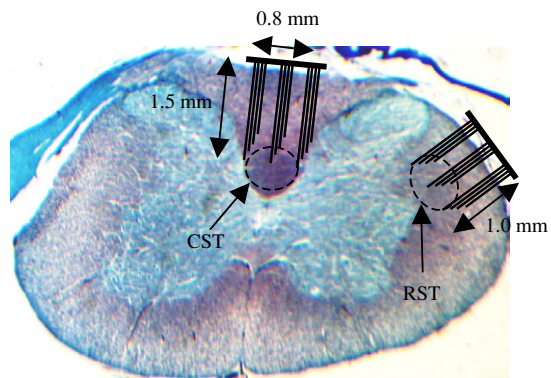


**Figure 1.** Cross-section of the C5–C6 spinal cord from one of the rats of this study stained using trichrome (gomori). Estimated locations of the CST and RST are marked. The electrode arrays are drawn on the same scale as the histology slide.

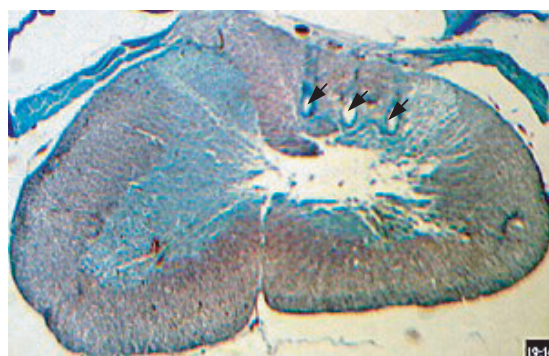


**Figure 2.** Histology section from one of the experimental animals at the C5–C7 level. The section is stained using trichrome (gomori blue). The arrows point the marks left by the electrode shanks in the right half of the dorsal column.

maintained by administering additional doses (20 mg kg<sup>-1</sup>, IP) as needed. Dexamethazone (2 mg kg<sup>-1</sup>, IM) was administered at the beginning of the surgical procedure to reduce secretions in the respiratory airways and CNS edema. The end-tidal CO<sub>2</sub> was monitored throughout the experiment. The animal's body temperature was maintained around 37 °C with the help of a heated-top surgical table. The back of the animal's neck was shaved and a skin incision was made along the midline. After C5–C7 laminectomy, electrodes were implanted either into the corticospinal or into the rubrospinal tracts in each animal. The dura was cut using a 26 g needle above the dorsal root entry zone. The spinocerebellar tract was severed with a scalpel in the medio-lateral direction to eliminate sensory traffic. Under microscopic vision (20 $\times$ ), the dorsal root entry zone was clearly visible on the spinal cord after removing the dura. Microelectrode arrays were implanted medial to the dorsal root entry zone (into the dorsal column) for recordings from the CST and lateral to the dorsal root entry zone (into the dorsolateral funiculus) for the RST, by gently pushing them into the cord to minimize the trauma. The estimated implantation sites for the electrodes are superimposed on the histology slide in figure 1. The histology section in figure 2

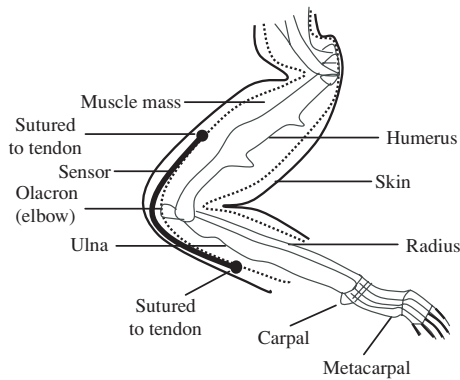


**Figure 3.** Positioning of the sensor on the rat's forelimb is shown. The sensor is attached to the tendons on both sides of the elbow joint.

shows the marks left by the actual implant from one of the animals.

A reference electrode was placed on the arachnoid surface. The electrodes were then covered by the transected dura and fixed in their respective positions using octyl cyanoacrylate tissue adhesive (Nexaband, WPI, Inc., FL). The skin was closed using size 5.0 absorbable sutures, and the 36-pin micro-connector of the electrode array was attached to the skin at the back of the animal using 4.0 non-absorbable sutures.

The upper limb was shaved and an incision was made on the dorsal side of the elbow to implant the flex sensor. The flex sensor was sutured to the tendons (figure 3) on both sides of the elbow joint on the dorsal aspect. After implantation, the skin was closed and the wires of the sensor were tunneled also to the back of the animal for connections. Antibiotic ointment and analgesics (Nubain,  $0.1 \text{ mg kg}^{-1}$ ) were used daily until the wounds healed completely.

### 2.3. Recording procedure

The rats were allowed to move freely in a transparent box during recording sessions. The box was placed inside a

Faraday cage for elimination of noise contamination from external sources. Cleaning the face with the forelimb behavior was studied, since this behavior involved cyclic movements of the forelimbs and it was easily generated without training. Seven-strand Teflon-coated stainless steel wires (A-M Systems, Inc., WA), bundled together as a cable, were used for connection between the animal and a 16-channel Grass amplifier (Warwick, RI). The wires were attached to a micro-connector header (H2761-ND, Digi-Key Corp., MN) on one end, which fitted into the connector on the animal's back, and a D-connector on the other for the amplifier. The connector cable was light-weight and flexible, which allowed the animal to move freely inside the cage. Recordings were made using the Grass amplifier set to a gain of 5000 and a pass-band of 100 Hz–6 kHz for all channels. The Grass amplifier was interfaced with the computer through a data acquisition card (NI-DAQ PCI-6071E, National Instruments) and LabView (National Instruments) at a sampling rate of  $40 \text{ k samples s}^{-1}$ .

### 2.4. Data analysis

Data analysis was performed using MATLAB (figure 4). Short episodes of data (1.5 s) were selected from the recordings. The power spectra of the raw signals were first plotted to determine if the signals contained sufficient neural components and also for proper selection of filter corner frequencies. A bandpass FIR filter (1–4 kHz) was first applied to the neural signals to remove some of the noise component. Principal component analysis was performed on the filtered neural signals. The elbow signal was filtered using a combination of elliptic and Butterworth filters. The combined filter pass-band was either 0–8 Hz or 4–8 Hz (see section 3). The same filter was also used for the integration of the rectified version of the principal neural components. Correlation coefficients between the neural and elbow signals were calculated. If the correlation on average was found to be larger than 0.8, then regression was performed on the neural components to reconstruct the elbow signal. A positive time delay of less than 100 ms in the elbow signal following the neural signal was considered as a motor activity.

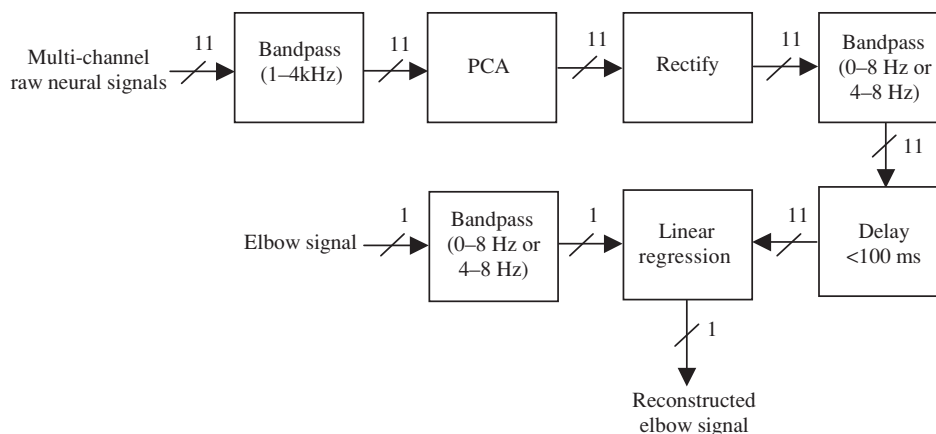


**Figure 4.** Flow diagram for data analysis. The numbers indicate the number of channels at each level of signal processing.

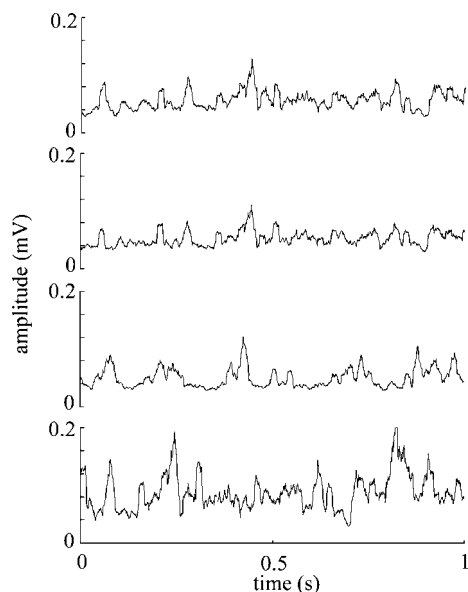


**Figure 5.** An episode of rectified-integrated neural signals extracted from the CST at the C5–C6 level using the microelectrode array (only four channels are shown).

Any reconstruction that occurred with a delay greater than 100 ms was discarded. The same signal processing paradigm was applied to the data recorded both from the CST and RST. A number of recording episodes used in the analysis distributed uniformly across the three animals. The flex sensor was calibrated by passively flexing the elbow of the animal in an anesthetized state and measuring the voltage output for a range of elbow angles.

### 3. Results

Electrode contact impedances were measured before (in normal saline) and after implantation at 2 kHz, and found to be in the range of 200–1500 k $\Omega$ . The impedances did not change substantially post-implantation, indicating that the contacts were intact and in place. A signal-to-noise ratio was calculated in the rectified-integrated neural signals and found to be approximately between 3 and 4 for both CST and RST signals. Figure 5 shows four channels of filtered and rectified-integrated neural signals recorded from the CST. Each channel has unique components although some waveforms appear in multiple channels.

The top four plots in figure 6 show the rectified-bandpass filtered version of the principal neural components. The bottom plot in figure 6 is the elbow signal from the flex sensor recorded simultaneously with the neural signals. At this stage, it is difficult to see a one-to-one correspondence between the neural and elbow signals because the elbow signal is controlled by a unique combination of the neural channels.

Reconstruction of the elbow signal with the neural signals extracted from the CST is shown in figure 7(A) and with the signals extracted from the RST in figure 7(B) for the frequency ranges of 0–8 Hz and 4–8 Hz.

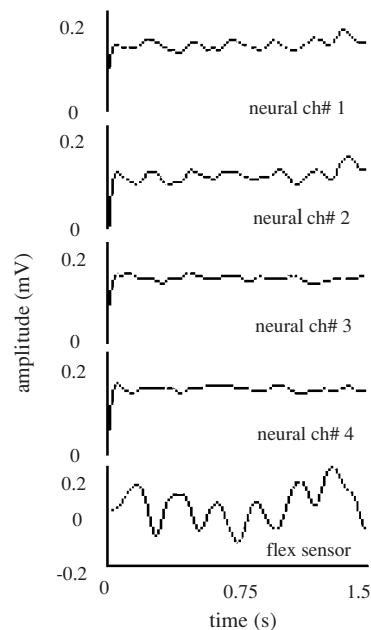


**Figure 6.** Rectified-bandpass filtered version of the principle components. Only four channels are plotted for clarity. The last channel shows the signal recorded from the sensor implanted on the elbow.

It can be observed in the reconstructed plots of figure 7 that the traces obtained as a result of linear regression closely follow the elbow signal. High values of correlation were found with positive time delays, as shown in table 1, between the reconstructed and actual elbow angles. In all episodes tested, both narrow band (4–8 Hz) and broader band (0–8 Hz) filtered signals performed equally in the reconstruction process (two-sided t-test,  $\alpha = 0.05$ ). The correlation coefficients obtained with the CST and RST signals were not significantly different (two-sided t-test,  $\alpha = 0.05$ ).

### 4. Discussion

In this study, the feasibility of extracting motor signals from the descending tracts of the cervical spinal cord in behaving rats and using these signals to reconstruct the arm movements was evaluated. Skilled reaching is widely thought to be unique to primates. Nevertheless, some other animals including the rats are equally adept in using a limb to reach and retrieve food. Thus, individual components of skilled limb movement have been widely used as a model to analyze a number of features of motor control [21–23]. Wishaw *et al* [24–26] showed that the components of reaching are similar in rats and humans by comparing their sequence and velocity profiles. This group also showed that both rats and humans moved the limb medially using the upper arm to aim it when they were required to reach through an aperture [26]. These similarities between the humans and rats in the use of upper extremities motivated our selection for the animal model.

In this study, the cervical segment C5–C6 of the spinal cord was chosen for the implantation of electrodes as the

**Table 1.** Mean correlation values between the measured and reconstructed elbow signals from the CST and RST.

	$F = 0.8 \text{ Hz}$		$F = 4\text{--}8 \text{ Hz}$	
	CST	RST	CST	RST
Number of episodes	14	8	20	12
Delay (ms)	$50 \pm 24.01$	$48.43 \pm 18.22$	$47.5 \pm 30.24$	$41.66 \pm 17.13$
Correlation coefficient	$0.90 \pm 0.04$	$0.89 \pm 0.03$	$0.85 \pm 0.05$	$0.85 \pm 0.05$

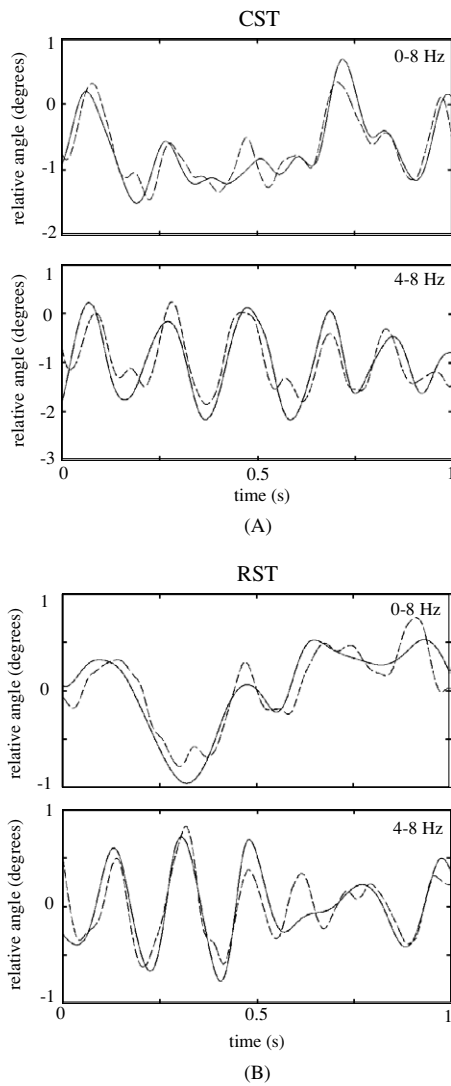


**Figure 7.** Reconstruction of the elbow signal using neural signals from the CST (A) and RST (B) for the filtering frequency ranges of 0–8 Hz (top trace) and 4–8 Hz (bottom) for different episodes of face cleaning behavior. The solid trace is the filtered elbow signal and the dashed trace is its reconstructed version from the principal neural components.

spinal roots exiting at these levels control the forearm. The RST and CST were selected for extraction of motor signals in this study. The RST and CST are believed to be involved in controlling the axial, distal and proximal musculature of the forelimb and digits in rats, primates and humans [21, 23, 25, 27–31]. However, the extent to which either of these

tracts is more functional for a particular motor task is still not known and debated equally. Therefore, electrodes were implanted on both RST and CST in different animals to study them comparatively. Our results do not favor one tract or the other for this simple behavior of face cleaning. Neither can we make a claim about the range of frequencies represented by each tract. Further experiments will have to be performed during detailed behavior of the animals to shed light on these questions.

It is impossible to completely isolate the RST signals from the sensory signals of the spinocerebellar tract due to the proximity of these neural pathways in the cord without severing the spinocerebellar tract. Sensory signals can significantly contaminate the motor signals and deteriorate the reconstruction process of the elbow movements. Cutting the spinocerebellar tract may have improved the reconstruction process. It should be noted that the sensory signals will not reach the proximal cord in a person with SCI and contaminate the motor signals. Therefore, severing the sensory pathways in this rat model does not contradict with the ultimate application of the technique in human subjects.

Impedances were measured prior to each recording session for the microelectrode array and found to be in the range of 200–1500 k $\Omega$ . The impedances were very low after a day or two post-operatively. However, the impedance values increased after 4–5 days when the acute response was complete. This reduction in impedance may be due to edema that occurs around the electrodes which remains for a few days after the surgical intervention. After this initial period, the impedance measures were found to be more or less constant for each electrode in the array while the recordings continued.

## 5. Conclusions

The results of this study demonstrate that motor signals can be extracted from the cervical spinal cord of behaving rats. It has also been shown that these motor signals can be used for reconstruction of the elbow joint movements. Future work involves increasing the number of contacts and hence the number of channels and to apply this paradigm to more complex behaviors.

## Acknowledgments

This study was supported by a Biomedical Engineering Research Grant from The Whitaker Foundation (RG-01–0366). Both authors were with Louisiana Tech University at the time of data collection.

## References

- [1] Chapin J K, Moxon K A, Markowitz R S and Nicolelis M A L 1999 Real-time control of a robot arm using simultaneously recorded neurons in the motor cortex *Nature Neurosci.* **2** 664–70
- [2] Nicolelis M A L, Ghazanfar A A, Faggin B M, Votaw S and Oliveira L M 1997 Reconstructing the engram: simultaneous, multisite, many single neuron recordings *Neuron* **18** 529–37
- [3] Hatsopoulos N G, Ojakangas C L, Paninski L and Donoghue J P 1998 Information about movement direction obtained from synchronous activity of motor cortical neurons *Neurobiology* **95** 15706–11
- [4] Laubach M, Wessberg J and Nicolelis M A L 2000 Cortical ensemble activity increasingly predicts behavior outcomes during learning of a motor task *Nature* **405** 567–71
- [5] Wolpaw J R, Birbaumer N, Heetderks W J, Mcfarland D J, Peckham P H, Schalk G, Donchin E, Quatrano L A, Robinson C J and Vaughan T M 2000 Brain-computer interface technology: A review of the first international meeting *IEEE Trans. Rehab. Eng.* **8** 164–73
- [6] Canedo A 1997 Primary motor cortex influences on the descending and ascending systems *Prog. Neurobiol.* **51** 287–335
- [7] Alstermak B, Kummel H, Pinter M J and Tantisira B 1990 Integration in descending motor pathways controlling the forelimb in the cat. 17. Axonal projection and termination of C3-C4 propriospinal neurons in the C6-Th1 segments *Exp. Brain Res.* **81** 447–61
- [8] Hongo T, Jankowska E and Lundberg A 1972 The rubrospinal tract: III. Effects on primary afferent terminals *Exp. Brain Res.* **15** 39–53
- [9] Terashima T 1995 Anatomy, development and lesion-induced plasticity of rodent corticospinal tract *Neurosci. Res.* **22** 139–61
- [10] Raineteau O, Fouad K, Bareyre F M and Schwab M E 2002 Reorganization of descending motor tracts in the rat spinal cord *Eur. J. Neurosci.* **16** 1761–71
- [11] Armand J 1982 The origin, course and terminations of corticospinal fibers in various mammals *Prog. Brain Res.* **57** 329–60
- [12] Brown L T Jr 1971 Projections and terminations of the corticospinal tract in rodents *Exp. Brain Res.* **13** 432–50
- [13] Miller M W 1987 The origin of corticospinal projection neurons in the rat *Exp. Brain Res.* **67** 339–51
- [14] Brosamle C and Schwab M E 1997 Cells of origin, course, and termination patterns of the ventral, uncrossed component of the mature rat corticospinal tract *J. Comp. Neurol.* **386** 293–303
- [15] Goodman D C, Jarrad L E and Nelson J F 1966 Corticospinal pathways and their sites of termination in the albino rat *Anatom. Rec.* **154** 462
- [16] Vahlsing H L and Feringa E R 1980 A ventral uncrossed corticospinal tract in the rat *Exp. Neurol.* **70** 282–7
- [17] Kuchler M, Fouad K, Weinmann O, Schwab M E and Raineteau O 2002 Red nucleus projections to distinct motor neuron pools in the rat spinal cord *J. Comp. Neurol.* **448** 349–59
- [18] Murray H M and Gurule M E 1979 Origin of the rubrospinal tract of the rat *Neurosci. Lett.* **14** 19–23
- [19] Branner A and Normann R A 2000 A multielectrode array for intrafascicular recording and stimulation in sciatic nerve of cats *Brain Res. Bull.* **51** 293–306
- [20] Aoyagi Y, Stein R B, Branner A, Pearson K G and Normann R A 2003 Capabilities of a penetrating microelectrode array for recording single units in dorsal root ganglia of the cat *J. Neurosci. Methods* **128** 9–20
- [21] Whishaw I Q, Gorny B P and Sarna J 1998 Paw and limb use in skilled and spontaneous reaching after pyramidal tract, red nucleus and combined lesions in the rat: behavioral and anatomical dissociations *Behav. Brain Res.* **93** 167–83
- [22] Schrimsher G W and Reier P J 1993 Forelimb motor performance following dorsal column, dorsolateral funiculi, or ventrolateral funiculi lesions of the cervical spinal cord in the rat *Exp. Neurol.* **120** 264–76
- [23] Whishaw I Q and Gorny B P 1996 Does the red nucleus provide the tonic support against which fractionated movements occur? A study on forepaw movements used in skilled reaching by the rat *Behav. Brain Res.* **74** 79–90
- [24] Whishaw I Q, Pellis S M, Gorny B P, Kolb B and Tetzlaff W 1993 Proximal and distal impairments in rat forelimb use in reaching follow unilateral pyramidal tract lesions *Behav. Brain Res.* **56** 59–76
- [25] Whishaw I Q, Pellis S M and Pellis V C 1992 A behavioral study of the contributions of cells and fibers of passage in the red nucleus of the rat to postural righting, skilled movements, and learning *Behav. Brain Res.* **52** 29–44
- [26] Whishaw I Q, Pellis S M and Gorny B 1992 Skilled reaching in rats and humans: evidence for parallel development or homology *Behav. Brain Res.* **47** 59–70
- [27] Kuypers H G J M 1964 The descending pathways to the spinal cord, their anatomy and function *Prog. Brain Res.* **11** 178–202
- [28] Lawrence D G and Kuypers H G J M 1968 The functional organization of the motor system in the monkey: I. The effects of bilateral pyramidal lesions *Brain* **9** 1–14
- [29] Kuypers H G J M 1981 Anatomy of the descending pathways *Handbook of Physiology. Section 1: The Nervous System* Vol II Motor Control, Part I (Bethesda, MD: American Physiological Society) pp 597–666
- [30] Hyland B 1998 Neural activity related to reaching and grasping in rostral and caudal regions of the rat motor cortex *Behav. Brain Res.* **94** 255–69
- [31] Jarratt H and Hyland B 1999 Neuronal activity in rat red nucleus during forelimb reach-to-grasp movements *Neuroscience* **88** 629–42